JFE TECHNICAL REPORT
No. 17 (Apr. 2012)

Various Measurement Technologies (Temperature/Stress/Fatigue/Crack) with Highly Precise Infrared Thermography and Their Applications†

NISHINA Yoshiaki[*1] IMANISHI Daisuke[*2] SHIBUYA Kiyoshi[*3]

Abstract:

Effective diagnostic technology of defects such as steel structures and machine parts has been developed by detecting a minute temperature change using highly precise infrared thermography, including the application of a thermoelasticity heat generation method to crack diagnosis and stress measurement. Also JFE Steel Group applied a supersonic wave excitation method to the crack diagnosis and we achieved various effective deterioration diagnoses in iron and steel manufacturing facilities. Some selected technologies have been currently applied to measurement business of JFE Steel Group.

1. Introduction

The JFE Steel Group is developing various measurement technologies utilizing highly precise infrared thermography as one effort to establish efficient diagnostic technologies. Highly precise, high speed measurement of extremely minute temperature changes by infrared thermography has become possible as a result of higher performance in infrared devices and measurement equipment and progress in signal processing technology. As a result, infrared thermography has evolved into a powerful diagnostic and measurement tool with a wide range of applications, not limited to conventional temperature measurement but extending to nondestructive inspections of stress, crack diagnosis, etc., and diverse examples of application have been reported[1)].

This paper introduces the principles of three techniques, i.e., the thermoelasticity heat generation method, the ultrasonic excitation method, and the thermo-wave method, as examples of measurement technologies using infrared thermography and their applications, development and application to high efficiency diagnosis of deterioration in steel works equipment, and development and application in the measurement business of the JFE Steel Group.

2. Crack Diagnosis and Stress Measurement Applying Thermoelasticity Heat Generation Method

2.1 Principle of Thermoelasticity Heat Generation Method[1)]

The temperature of a gas decreases when adiabatic expansion occurs, and conversely, its temperature increases under adiabatic compression. In solids, a similar phenomenon is known to occur as a result of sudden stress. This is generally called the thermoelasticity effect. In metals and other homogeneous materials, heat generation by the thermoelasticity effect can be expressed by Eq. (1)[2,3)].

$$\Delta T = -K \cdot T \cdot \Delta\sigma \quad \cdots\cdots (1)$$

where, $\Delta\sigma$ is the change in the sum of principal stresses,

---

† Originally published in *JFE GIHO* No. 27 (Feb. 2011), p. 9–14

*1 Senior Researcher Manager,
Mechanical Engineering Res. Dept.,
Steel Res. Lab.,
JFE Steel

*2 Mechanical Engineering Res. Dept.,
Steel Res. Lab.,
JFE Steel

*3 Project General Manager,
Sensing & Visualization Analysys Center,
Solution Div. (Kawasaki),
JFE Techno-Research

T is absolute temperature, and K is the thermoelastic coefficient. The thermoelastic coefficient is a characteristic value of each material, and for mild steel, $K = 3.5 \times 10^{-12}$ Pa^{-1}.

In crack diagnosis and stress measurement using the thermoelasticity effect in Eq. (1), the minute temperature change when a stress change occurs in the object of measurement is measured by highly precise infrared thermography (temperature resolution: 0.02 K), and the stress value is then calculated based on Eq. (1). When a crack exists in the object of measurement, a stress concentration will occur at the tip of the crack, and it is possible to detect the crack as a temperature anomaly. The next section introduces the self reference lock-in method, which is a signal processing method that is applied to improve measurement accuracy.

2.2 Basic Principle of Self Reference Lock-in Method [1,4)]

Figure 1 shows schematic diagrams of models of the conventional lock-in method and the self reference lock-in method used in this paper. The conventional lock-in method is a signal processing method in which a reference signal such as a load signal, etc. is obtained from the tester, a signal with the same frequency as the reference signal is extracted from the time-series change measured by infrared thermography, and the *S/N* ratio (signal to noise ratio) is improved. However, application to actual equipment is difficult because random stresses act on the object of measurement, and there are also many cases in which a load signal cannot be obtained as a reference signal. On the other hand, the self reference lock-in method uses temperature changes in a reference area in the infrared image. As described in the previous section, a linear correlation exists between stress change (load change) and temperature change. This means their change frequencies are the same. Therefore, even in cases where a load signal cannot be obtained, as in actual equipment, it is possible to obtain an *S/N* improvement effect similar to that in lock-in processing by using the temperature change in the infrared image as a reference signal.

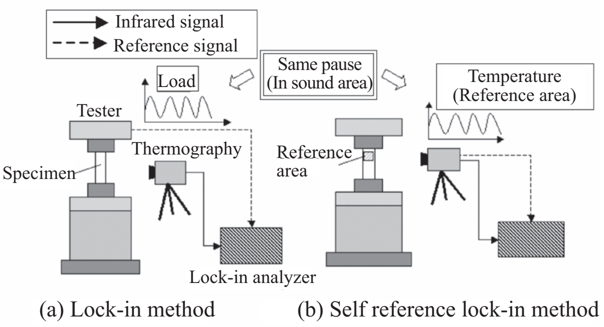

Fig. 1 Schematic illustration of signal processing method

2.3 Crack Diagnosis Applying Thermoelasticity Heat Generation Method [5,6)]

This section introduces the development of a crack diagnosis method applying infrared thermography to improve equipment diagnosis efficiency in the steel works, together with an example of its application. First, the thermoelasticity heat generation method is verified and the minimum stress necessary for crack detection is investigated using a test sample prepared by partially cutting an actual crane girder. A schematic illustration of the test is shown in **Fig. 2**. A fatigue crack was introduced in the weld toe of the triangular rib of the cut sample. A stress waveform which attenuated while vibrating from a stress amplitude of 100 MPa to 10 MPa was loaded on this sample using a sine waveform with a frequency of 2 Hz. Infrared thermography measurement was performed at a distance of 15.3 m from the object of measurement using a telephoto lens with a focal length of 200 mm. The acting stress was measured by attaching a strain gauge to the test sample.

Figure 3 shows the stress distribution images at stress amplitudes of 100 MPa, 50 MPa, 20 MPa, and

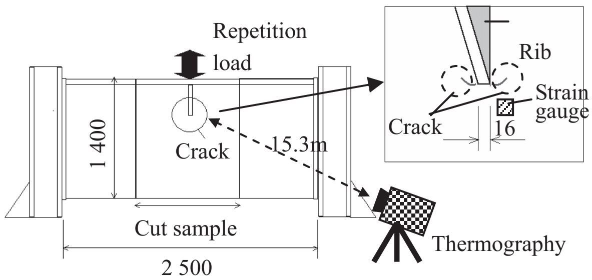

Fig. 2 Schematic illustration of the test in the laboratory (Offline test)

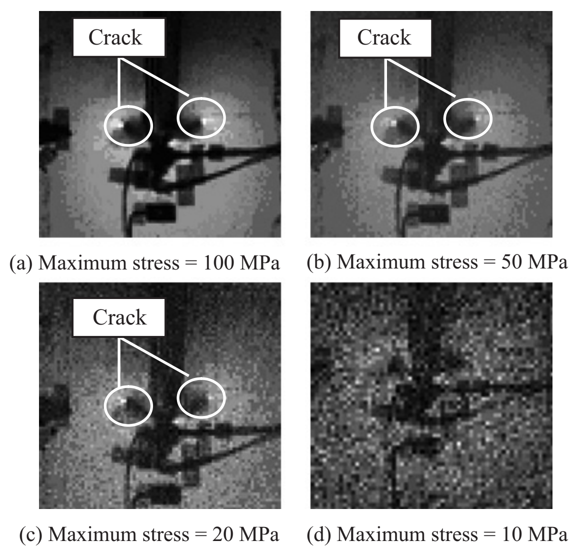

Fig. 3 Infrared image around cracks in various stress applied (100, 50, 20, and 10 MPa)

10 MPa. The results of this experiment verified that the crack tip can be detected as a high temperature parts (shown in white) in the crack areas (areas surrounded by solid lines in Fig. 3). Next, **Fig. 4** shows the results of verification of the thermoelasticity effect by obtaining the correlation of stress amplitude and temperature rise. The straight line is a theoretical solution for the thermoelasticity effect shown by Eq. (1). As the plots for stress and temperature rise are approximately on the straight line showing the theoretical solution, it can be understood temperature rise can be converted to stress with good accuracy.

Based on the results obtained in the laboratory tests, as described above, a remote crack diagnosis test was performed by applying this method to a box beam girder of an overhead traveling crane that was scheduled for repair. A schematic illustration of this test is shown in **Fig. 5**. A crab trolley is mounted on the girder for load hoisting, and traversing is possible. The load acting on the wheels of the crab trolley is the total of the dead weight of the trolley and the suspended load (80% of rated load). The stress fluctuations acting on the girder were measured by an infrared thermograph installed on the ground while changing the stress acting on the girder as the crab trolley traversed the girder several times. The distance between the measurement surface and the infrared thermograph on the ground was approximately 23 m.

An overall view of a stress distribution image measured with the infrared thermograph is shown in **Fig. 6** (a), and an enlargement of the crack area is shown in Fig. 6 (b). Positions of high stress (areas shown in white), where the stress concentration on the crack can be seen as a factor, were detected on the right side of the triangular rib (area surrounded by solid line). **Figure 7** shows the stress-line profile in the crack area shown in Fig. 6 (b). As stress increases sharply at crack tip (α) and crack tip (β), the stress concentration on the crack can be measured clearly. On the other hand, the stress

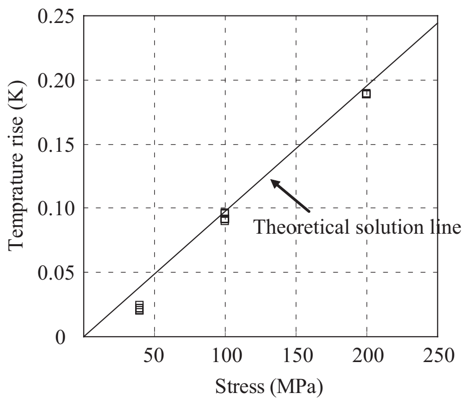

Fig. 4 Relationship between stresses measured by strain gauge and temperature rise

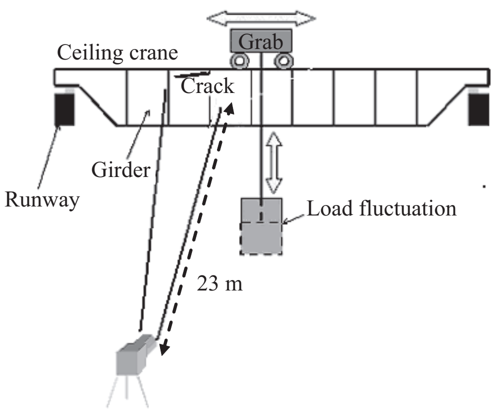

Fig. 5 Schematic illustration of online test (Box beam girder of overhead crane system)

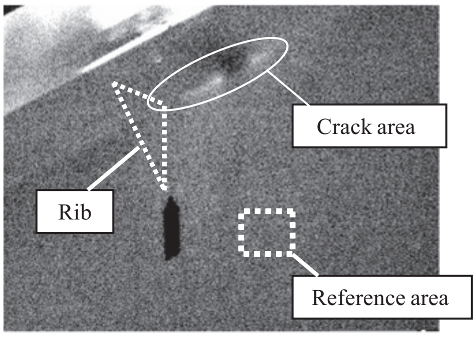

(a) Image of stress distribute in box beam girder

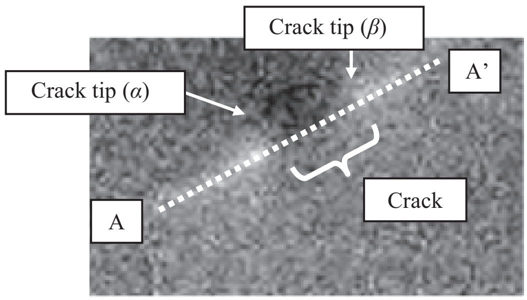

(b) Expanded image of crack area shown in (a)

Fig. 6 Image of stress distribute in box beam girder of overhead crane system (No signal processing)

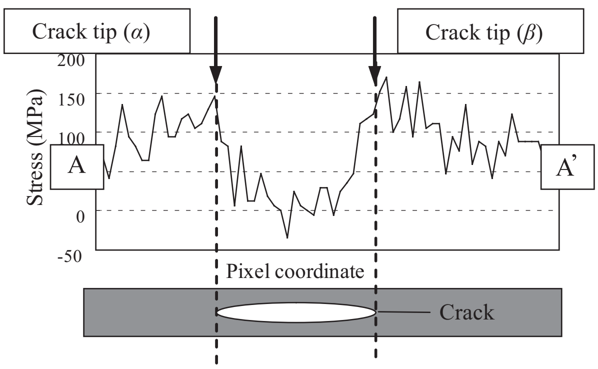

Fig. 7 Stress line-profile in line A-A' shown in Fig. 6 (b)

between the two crack tips was virtually zero, showing that neither compression nor tension acted on that area. This is because the crack opening is not mechanically constrained except at the crack tip and strain does not act in the area.

Next, **Fig. 8** shows the time-series stress change measured by infrared thermography. It can be understood that stresses from 30 MPa to approximately 80 MPa acted on the sound part (reference area in Fig. 6) when the crab trolley passed over the measurement area 3 times. The stress under the 80% loading condition in this test was calculated at 30–60 MPa by finite element method (FEM) analysis, showing that it is possible to measure stress with good accuracy. On the other hand, large stresses from 100 MPa to 180 MPa acted on the crack tip due to stress concentration. In the stress curve for the crack tip, two peaks were detected in each pass. This shows that stress reached its maximum in the instant when the two wheels of the crab trolley passed over the crack tip.

As described above, it is possible to obtain the crack length from 2-dimensional data and stress fluctuations from time-series change data.

Figure 9 shows the results of improvement of the *S/N* ratio using the self reference lock-in method described in Section 2.2. The stress fluctuation of the reference area in Fig. 6 (a) was used as the reference signal. The *S/N* ratio improved remarkably, and it was also possible to detect crack tip heat generation at the tip of the triangular rib.

As shown by this explanation, the possibility of remote crack diagnosis of a crane structure by the thermoelasticity heat generation method using loading fluctuations of the force was verified. Further verification is planned for the future.

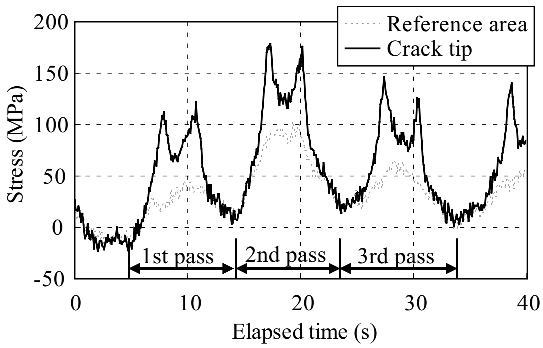

Fig. 8 Comparison of Stress change between crack tip and sound area ("Reference area" shown in Fig. 6 (a))

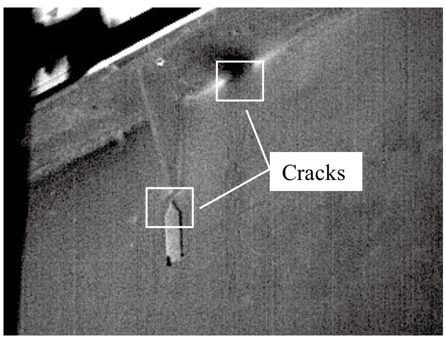

Fig. 9 Image of stress distribute after signal processing (Self reference lock-in method)

2.4 Stress Measurement Applying Thermoelasticity Heat Generation Method

This section introduces an example of stress distribution measurement of multi-stage spot welds using the thermoelasticity heat generation method as an example of development and application in measurement business of JFE Steel Group. **Figure 10** (a) shows a stress distribution image of a spot weld. Fig. 10 (b) shows the stress profiles of lines ①, ②, and ③ in (a). At the entrance side of spot welding of the first stage, the peaks of tensile stress follow line ①, but at welding line ② of the 2nd stage spot welding arranged at the exit side of the first stage, the peaks of compressive stress are followed with the phases (peaks and valleys) reversed from those in line ①. If the two sheets are pulled upward and downward, rotary bending force is generated in the surfaces. In this case, along the line ②, top surface of the welded sheet is mainly subjected to compression, and tensile stress is mainly generated on the back surface of the other sheet. In line ③, which is at a distance from

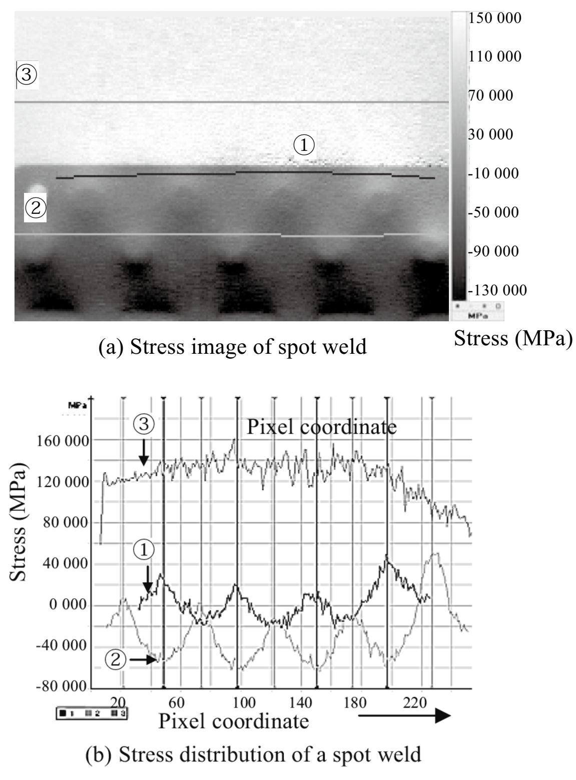

(a) Stress image of spot weld

(b) Stress distribution of a spot weld

Fig. 10 Example of stress measurement result the weld, a slight load deviation can be observed on the right side, but the generated stress is mild and homogeneous. As this example demonstrates, complex phenomena such as the division of stresses between sheets in spot welding, friction between the sheets, etc. can be observed by 2-dimensional images.

3. Crack Diagnosis Using Ultrasonic Excitation Method

3.1 Basic Principle of Ultrasonic Excitation Method

With the thermoelasticity heat generation method explained in Chapter 2, it is necessary to apply external stress to the object of inspection. This section introduces an example of the development and application of an ultrasonic excitation method[7] as a crack diagnosis method for equipment in a static condition, such as rolls when lines are not in operation. In this method, ultrasonic vibration is irradiated on the object of measurement so as to generate frictional heat at the crack surface, and minute temperature changes are measured by infrared thermography.

3.2 Results of Laboratory Crack Detection Tests

A test specimen was prepared by introducing an artificial crack (length: 10 mm, depth: 5 mm) in a flat plate (100 mm × 200 mm), and the relationship between crack heat generation and the press load of the ultrasonic horn and the amplitude of the irradiated ultrasonic wave was investigated. The frequency of the irradiated ultrasonic wave was 19.5 kHz. As shown in **Fig. 11**, temperature rise (crack heat generation) increases when the press load of the ultrasonic horn is increased. This is estimated to be because contact between the horn and the specimen surface is improved, and irradiation loss of the ultrasonic vibration is reduced. From **Fig. 12**, temperature rise also increases when the amplitude of the irradiated vibration is increased. This is estimated to occur

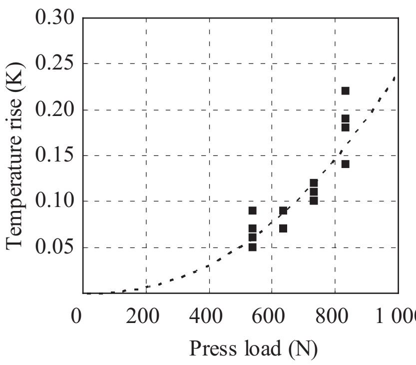

Fig. 11 Relationship between press load of ultrasonic horn and temperature rise (Plate specimen)

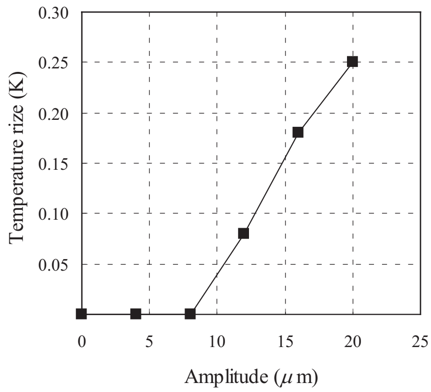

Fig. 12 Relationship between amplitude of ultrasonic horn and temperature rise (Plate specimen)

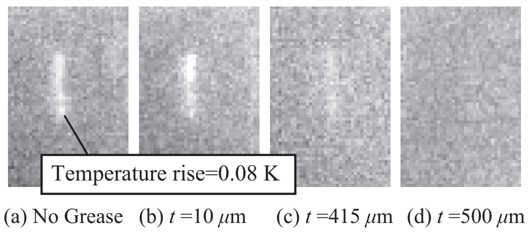

Fig. 13 Affection of grease in crack detestability (Crack length = 10 mm, Depth = 5 mm)

because the vibration amplitude of the crack surface increases, and as a result, frictional heat generation at the crack surface is increased.

Next, the effect of grease contamination on crack detection capacity was evaluated, as grease is an issue when this technology is applied at actual worksites. Detection tests were performed with test specimens coated with various film thicknesses of mechanical grease. **Figure 13** shows the results. Without grease, the temperature rise due to the crack is 0.08 K. Crack detection was impossible when the grease thickness exceeded an average of 500 μm. However, after simple wiping to remove the grease, the film thickness was reduced to no more than 10 μm, and crack detectability was verified.

3.3 Demonstration Test of Crack Detection in Table Roll Neck Part

Using this technique, a fatigue crack detection test was performed on the neck part of a table roll which was scheduled for reconditioning. A schematic illustration of the test is shown in **Fig. 14**. Cracks had occurred at two spots on the stepped part of the roll. The distances between the ultrasonic vibrator and the cracks in the stepped part were 500 mm for crack A and 630 mm for crack B. The crack size was 68–76 mm in length and 25–32 mm in depth. Initially, the vibrator (vibration frequency: 19.5 Hz) was installed on the roll barrel (500 mm in dia.), and the changes in temperature at

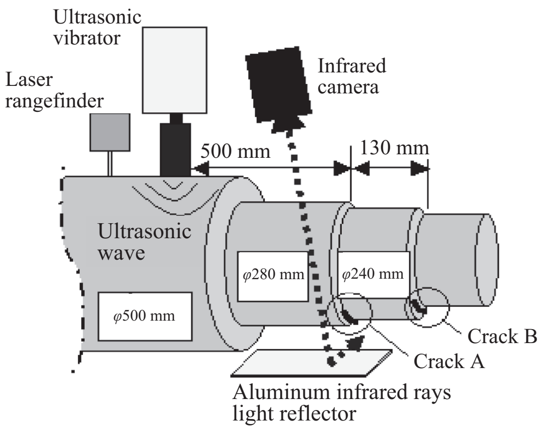

Fig. 14 Schematic illustration of defecting cracks in table roll

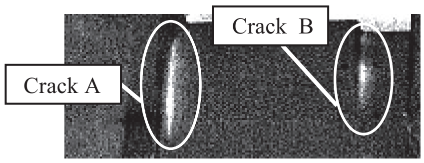

Fig. 15 Infrared image in table roller neck part (Self reference lock-in method)

crack A and crack B were measured by infrared thermography. An aluminum infrared light reflector (infrared light reflection: 90% or more) was used to measure cracks on the bottom side of the stepped part. **Figure 15** shows the results of the infrared image after self reference lock-in processing. As reference signals, the ultrasonic horn and part irradiated with ultrasonic vibration were used.

As can be seen in Fig. 15, the cracked parts were detected as high temperature parts (white parts). By using the aluminum infrared light reflector, it was also possible to measure parts which could not be measured by direct infrared thermography. The range of angle of one measurement is 100° of the roll neck circumference, which means it is possible to measure the entire circumference by rotating the roll 3 times. As the detection range in one measurement operation is larger than with the conventional method, a large reduction in the measurement time required per roll is possible.

JFE Steel has begun practical application of this ultrasonic excitation method at its steel works, contributing to improved inspection efficiency, which was an original target. Moreover, because it is now possible to perform crack inspections of parts which were difficult to measure with the conventional method, this method is also contributing to prevention of equipment trouble due to fatigue fracture.

4. Internal Defect Diagnosis Applying the Thermo-Wave Method

This chapter introduces an example of internal defect diagnosis using the thermo-wave method as an example of development and application in measurement business of JFE Steel Group. This is a method in which the object being inspected is heated cyclically with a heating lamp or the like. As shown in **Fig. 16**, an internal crack (defect) or inhomogeneity of the material will cause a difference in thermal diffusivity, which in turn causes a difference in the transmission time of the heat wave passing through the part. This is measured by highly precise infrared thermography, and the location of the defect is displayed by preparing a 2-dimensional image of the distribution of thermal diffusivity using Eq. (2) which is derived from a thermal diffusion equation. Here, a: thermal diffusivity, f: heating frequency, d: plate thickness, $\Delta\theta$: phase difference, λ: thermal conductivity, C_p: specific heat at constant pressure, and ρ: density. The principle is the thermal wave method in ISO 22007-3. In addition to defect detection, this method is also used in measurements of the thermal diffusivity and thermal conductivity of large-scale parts which cannot be measured by the laser flash method.

$$a = \pi \cdot f \cdot \left(\frac{d}{\Delta\theta + \frac{\pi}{4}} \right)^2 \quad \cdots\cdots (2)$$

$$\lambda = a \cdot C_p \cdot \rho \quad \cdots\cdots (3)$$

Although mechanical, chemical, and thermal loads cause deterioration in the materials used in cells such as

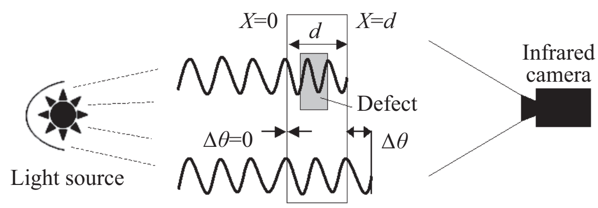

Fig. 16 Measurement principle of thermo-wave method

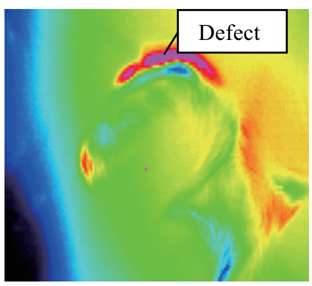

Fig. 17 Example of the defect in plastic film

secondary cells, fuel cells, solar cells, etc., this can be detected as a change in thermal properties. **Figure 17** shows an example in which an internal defect in a plastic film was diagnosed by the thermo-wave method. An area (shown in red) where thermal diffusivity has been extremely reduced by deterioration can be observed.

5. Conclusion

This paper introduced examples of the development and application of various measurement technologies utilizing infrared thermography from the viewpoint of establishing efficient deterioration diagnosis technologies. At JFE Steel, effective use of a combination of these developed technologies at the company's steel works has made it possible to carry out appropriate renovations based on a quantitative evaluation of the degree of deterioration in the object equipment, resulting in stable equipment operation. Further, JFE Techno-Research uses highly precise infrared thermography in commissioned measurements/development support and sells a system development product (trade name: Thermo-Tec), and has received a high evaluation from clients.

References

1) Sakagami, Takahide. Recent Progress in Nondestructive Evaluation Techniques Using Infrared Thermography. Hihakaikensa. 2002, vol. 51, no. 6, p. 321–327.
2) Wu, Datong; Salerno, Antonio. "Phase Sensitive Modulation Thermography and Its Application for NDE." Proceedings of SPIE. vol. 3056, p. 176–183.
3) Xavier, P. V. Maldague. "Theory and Practice of Infrared Technology for Nondestructive Testing."
4) Lesniak, Jon R.; Boyce, Brad R. "Thermo-elastic measurement under random loading." Proc. of the SEM Spring Conf. On Experimental and Applied Mechanics and Experimental/Numerical Mechanics in Electronic Packaging Ⅲ. Soc. for Exp. Mech. 504-507, 1998-06.
5) Sakagami, Takahide; Sakino, Yoshihiro; Nishimura, Takashi; Kubo, Shiro. Ishino, Kazushige; Kurihara, Yasuyuki. Proceedings of the 60th Annual Conference of the Japan Society of Civil Engineers. 2005, p. 123–124.
6) Sakagami, Takahide; Nishimura, Takashi; Kubo, Shiro; Sakino, Yoshihiro; Ishino, Kazushige. Development of a Self-reference Lock-in Thermography for Remote Nondestructive Testing of Fatigue Crack: 1st Report, Fundamental Study Using Welded Steel Samples. Transactions of the Japan Society of Mechanical Engineers, Series A. 2006-12, vol. 72, no. 724, p. 1860–1867.
7) Murase, Morimasa; Sukigara, Nao; Tamayama, Tiga; Okumura, Takeru; Yasui, Makoto; Kawashima, Koichiro. Detection of tight cracks with thermo-sonic method. Proceedings of the 2004 Annual Meeting of the JSME/MMD. 2004, p. 93–94.